

# Self-Confirming Transformer for Locally Consistent Online Adaptation in Multi-Agent Reinforcement Learning

Tao Li\*, Juan Guevara, Xinghong Xie, and Quanyan Zhu

Department of Electrical and Computer Engineering, New York University  
 {t12636, jdq8833, xx2233, qz494}@nyu.edu

## Abstract

Offline reinforcement learning (RL) leverages previously collected data to extract policies that return satisfying performance in online environments. However, offline RL suffers from the distribution shift between the offline dataset and the online environment. In the multi-agent RL (MARL) setting, this distribution shift may arise from the nonstationary opponents (exogenous agents beyond control) in the online testing who display distinct behaviors from those recorded in the offline dataset. Hence, the key to the broader deployment of offline MARL is the online adaptation to nonstationary opponents. Recent advances in large language models have demonstrated the surprising generalization ability of the transformer architecture in sequence modeling, which prompts one to wonder *whether the offline-trained transformer policy adapts to nonstationary opponents during online testing*. This work proposes the self-confirming loss (SCL) in offline transformer training to address the online nonstationarity, which is motivated by the self-confirming equilibrium (SCE) in game theory. The gist is that the transformer learns to predict the opponents' future moves based on which it acts accordingly. As a weaker variant of Nash equilibrium (NE), SCE (equivalently, SCL) only requires local consistency: the agent's local observations do not deviate from its conjectures, leading to a more adaptable policy than the one dictated by NE focusing on global optimality. We evaluate the online adaptability of the self-confirming transformer (SCT) by playing against nonstationary opponents employing a variety of policies, from the random one to the benchmark MARL policies. Experimental results demonstrate that SCT can adapt to nonstationary opponents online, achieving higher returns than vanilla transformers and offline MARL baselines.

## Introduction

Offline reinforcement learning (RL) has recently emerged as a promising alternative to online RL (Levine et al. 2020), which extracts policies purely from the previously collected dataset without any interaction with the environment. As such, offline RL avoids online explorations required by online RL algorithms, which can be expensive (e.g., end-to-end robotic control (Károly et al. 2021)), dangerous (e.g., self-driving (Li, Lei, and Zhu 2023)), and sometimes infeasible (e.g., healthcare (Yu et al. 2021)).

\*Corresponding author

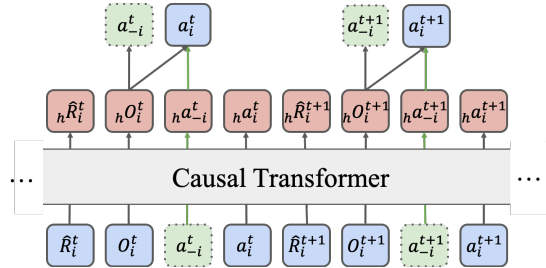


Figure 1: Self-Confirming Transformer (SCT) architecture. SCT first generates a conjecture on the opponent's action  $a_{-i}^t$  (the green block) based on the hidden state  $hO_i^t$  of the observation  $O_i^t$  produced by the transformer. This conjecture (or equivalently, its hidden state  $ha_{-i}^t$ ), together with the observation hidden state  $hO_i^t$ , leads to the agent's action generation  $a_i^t$  (the green arrow). The offline trained SCT enables the agent to reason its opponent's move in online testing.

Yet, a fundamental challenge of offline RL is the distribution shift between the offline training dataset and the online testing environment (Levine et al. 2020). In plain words, the offline RL agent needs to properly handle unseen state-action pairs in the dataset during testing (Bannon et al. 2020). When extending this offline RL framework to multi-agent RL (MARL) settings, the distribution shift may be caused by exogenous agents who are beyond the preview of the trained MARL policy. We refer to these exogenous agents as the opponents. When opponents display a behavior pattern different from those included in the offline dataset, the ego agents, controlled by the learned MARL policy, are unprepared for these unseen state-action pairs resulting from opponents' unexpected moves. We refer to such an opponent as nonstationary, as it employs a different and possibly time-varying policy in testing, as opposed to the stationary policy used to collect offline data. As shown in one motivating example presented in Figure 3, blindly applying offline MARL policy gives degrading performance when playing with a nonstationary opponent.

We refer to such a phenomenon as the curse of the nonstationary opponent, which we believe is relevant to many offline MARL problems. Take human-robot interaction (HRI) as an example. In this context, the robot acts as the peer, companion, or even adversary (Mutlu, Roy, and Šabanović

2016) of humans who are beyond the robot’s direct control. Moreover, as personalities, capabilities, and cognitive levels vary across different people, it is intractable to build a universal human behavioral model that can be used in offline training. Hence, the human becomes the nonstationary opponent in HRI, if the robot is exposed to one whose behavior pattern is missing in the dataset.

Given the significance and relevance of this curse in MARL, this work explores the possibility of transforming offline MARL into a sequence modeling problem and addresses this curse using the Transformer architecture (Vaswani et al. 2017) that has exhibited surprising generalization in large language models (Radford et al. 2018). The question we ask is *whether the transformer policy learned from offline data can generalize/ adapt to the nonstationary opponent online*.

This work answers this question affirmatively by introducing the self-confirming transformer (SCT) that learns to predict the opponent’s move from the partial observation, which is then fed to the transformer itself to generate the ego agent’s action, as depicted in Figure 1. The SCT is inspired by the self-confirming equilibrium (SCE) (Fudenberg and Levine 1993), a weaker variant of the seminal Nash equilibrium (NE) (Nash 1951). NE is a global notion built on collective rationality (see (1)), requiring every agent’s compliance to deliver optimality. In contrast, SCE rests on subjective rationality, focusing on local consistency between one’s observations and subjective conjectures on the opponent’s future move, which leads to the term “self-confirming” (see Definition 1). The intuition of adopting SCT is that offline data is collected using benchmark MARL policies (assumed to be NE), from which the transformer learns to play the equilibrium policy online under the wrong belief that other agents also use NE policies. In contrast, local consistency learned offline helps adjust the agent’s belief according to the online observations. From an offline RL perspective, local consistency prevents the transformer from overfitting the offline data, creating online adaptability. Our contributions are as follows.

- We empirically present the curse of the nonstationary opponent that degrades offline MARL policies.
- We propose the self-confirming transformer (SCT) with the learning objective shifted from global optimality indicated by NE to local consistency of SCE to address the curse of the nonstationary opponent.
- We conduct extensive experiments in benchmark MARL environments to compare SCT with offline MARL baselines and recent transformer-based methods, where SCT demonstrates comparatively decent online adaptability.

## Related Works

**MARL** A large body of prior MARL works has investigated the online paradigm, where multiple agents can interact with the environment. To address the learning instability brought by this multi-agent simultaneous interaction, the framework of centralized training with decentralized execution (CTDE) is introduced in (Lowe et al. 2017), where a centralized critic is trained to gather all agents’ local

information and evaluate individual policies. CTDE leads to many successful MARL developments, including multi-agent policy gradient methods (Foerster et al. 2018; Lowe et al. 2017) and value-decomposition methods (Rashid et al. 2020; Sunehag et al. 2018).

**Offline RL** Unlike online RL, such as TD-learning (Sutton, Maei, and Szepesvári 2009; Li and Zhu 2019), requiring repeated interactions, offline RL policy is learned from an offline dataset collected by CTDE. One fundamental question in offline RL is the distribution shift (Levine et al. 2020). To address this issue, recent progress utilizes the conservatism idea (Levine et al. 2020) that compels the policy (Fujimoto and Gu 2021) or value function estimation (Kumar et al. 2020; Fujimoto, Meger, and Precup 2019) to the data manifold. Our work focuses on a particular case of the distribution shift caused by the nonstationary opponent. Instead of incorporating conservatism into offline training as in (Pan et al. 2022), we explore a game-theoretic approach to equip the agent with online adaptability, harnessing the generalization power of the transformer architecture.

**Transformer** The transformer is originally proposed for sequence modeling problems in natural language processing (Vaswani et al. 2017). The recent trend of treating offline RL as a sequence modeling problem and applying transformer policies has produced encouraging success. The decision transformer (Chen et al. 2021) and the trajectory transformer (Janner, Li, and Levine 2022) outperform many state-of-the-art offline RL algorithms, which tackle the credit assignment and trajectory prediction problems using self-attention (Vaswani et al. 2017). The current multi-agent transformer research (Wen et al. 2022; Meng et al. 2023) concentrates on cooperative tasks: all agents are controlled by a central transformer. We leverage a novel transformer to handle nonstationary opponents in noncooperative settings.

## Offline Multi-Agent Reinforcement Learning

### Multi-Agent Reinforcement Learning

**MARL as Markov Games** Consider learning in a multi-agent decision process described by a partially observable Markov game (POMG). A POMG with  $N$  agents indexed by  $i \in \{1, 2, \dots, N\} := [N]$  includes a global state space  $\mathcal{S}$ , each agent’s action space  $\mathcal{A}_i$ , and a set of observations  $\mathcal{O}_i$  for each individual. The typical elements of these spaces are denoted by the corresponding uncapitalized letters. The time step is denoted by  $t \in \mathbb{N}_+$  appearing as the superscript in the sequel. Unaware of the global state  $s^t$ , each agent receives a local observation  $o_i^t \in \mathcal{O}_i$  and chooses an action  $a_i^t$ . Then, with the joint actions of all agents, denoted by the bold symbol  $\mathbf{a}^t = (a_1^t, a_2^t, \dots, a_N^t)$ , the environment transits to the next state  $s^{t+1}$  according to the transition kernel  $\mathcal{P} : \mathcal{S} \times \prod_{i \in [N]} \mathcal{A}_i \rightarrow \Delta(\mathcal{S})$ , and the decision-making process repeat. We assume all involved sets in this work are Borel sets (either discrete or continuous), and  $\Delta(\cdot)$  denotes the Borel probability measure. To be specific,  $\mathcal{P}(s^{t+1}|s^t, \mathbf{a}^t)$  give the distribution of the next state.

Agent’s performance is evaluated through the reward function  $r_i : \mathcal{S} \times \prod_{i \in [N]} \mathcal{A}_i \rightarrow \mathbb{R}$ , and each agent aims

to maximize its own discounted return  $\sum_{t=1}^T \gamma^t r_i^t$ , where  $r_i^t = r_i(s^t, \mathbf{a}^t)$ , and  $T$  denotes the horizon length. The agent’s information set or structure  $\mathcal{I}_i^t$  captures the environmental feedback that helps the agent identify the policy improvement direction (Li, Zhao, and Zhu 2022). We consider the conventional decentralized information set, consisting of local feedback:  $\mathcal{I}_i^t = \{o_i^t, a_i^t, r_i^t\}$  in a non-cooperative multi-agent environment, including competitive and mixed cooperative-competitive scenarios (Lowe et al. 2017), where agents may have distinct reward signals, i.e.,  $r_i \neq r_j$  for some  $i, j \in [N]$ .

Each agent aims to find a policy  $\pi_i \in \Pi_i$  that maps the information set to some action at each time step:  $a_i^t \sim \pi_i(\cdot | \mathcal{I}_i^t)$  to maximize the discounted return, where  $\pi_i$  is assumed to be a stochastic policy yielding a distribution on  $\mathcal{A}_i$ . We use  $\pi_i$  and  $\theta_i$  interchangeably to refer to the agent’s policy. Let  $\boldsymbol{\pi} = (\pi_1, \pi_2, \dots, \pi_N)$  be the joint policy of all agents, where each policy  $\pi_i$  is parameterized by  $\theta_i \in \Theta_i$ ,  $i \in [N]$ . The following discussion uses bold symbols, such as  $\mathbf{a}$  and  $\mathbf{o}$ , to denote the joint quantities. In addition, we use the subscript  $-i$  (e.g.,  $\pi_{-i}$  and  $a_{-i}$ ) to denote some joint quantity of all but the agent  $i$ .

### Centralized Training with Decentralized Execution

Given the joint policy  $\boldsymbol{\theta}$ , the agent  $i$ ’s expected return is  $J_i(\theta_i, \theta_{-i}) = \mathbb{E}_{a_i^t \sim \pi_i, a_{-i}^t \sim \pi_{-i}} [\sum_{t=1}^T r_i(s^t, a_i^t, a_{-i}^t)]$ , where the other agents’ policies also play a part. Hence, when determining the optimal policy, one must consider other agents’ policies, as one’s performance intertwines with others’ moves. This interdependency leads to Nash equilibrium (NE) (Nash 1951) as the solution concept in non-cooperative settings, where the agents’ optimal policy  $\pi_i^*$  or  $\theta_i^*$  is characterized by the “no-incentive-to-deviate” principle:

$$J_i(\theta_i^*, \theta_{-i}^*) \geq J_i(\theta_i', \theta_{-i}^*), \forall i \in [N], \forall \theta_i' \in \Theta_i. \quad (1)$$

As one can see from (1), NE indicates the global optimality in the sense that the optimality of each individual policy  $\theta_i^*$  from (1) rests on the assumption that every other agent conforms with NE as well. We refer to this assumption as *collective rationality*. The collective rationality originates from the interdependent nature of multi-agent decision-making that prompts each agent to reason their opponents’ decision-making so as to maximize the return. However, such reasoning needs global/centralized information set than the decentralized one considered above, which includes observations of opponents. Using RL language, incorporating global information  $\mathcal{I}_g^t = \{s, (o_i^t, a_i^t, r_i^t)_{i \in [N]}\}$  helps each agent cope with the environmental nonstationarity resulting from other agents’ actions in the training phase. The idea of augmenting agent’s information set with global information leads to the widely received MARL framework of centralized training with decentralized execution (CTDE). In CTDE, agents are trained in a centralized manner where they can access  $\mathcal{I}_g^t$  to learn a decentralized policy to be implemented during testing, which only requires local feedback, e.g.,  $\pi_i(\cdot | o_i^t)$ .

Even though CTDE belongs to the online MARL paradigm, seemingly detached from our offline RL study, we observe that CTDE has been widely adopted to collect datasets for offline MARL research (Pan et al. 2022;

Meng et al. 2023; Tseng et al. 2022). The common practice of collecting offline data using CTDE proceeds as follows. First, one selects a benchmark online MARL algorithm, such as MADDPG (Lowe et al. 2017) and MATD3 (Ackermann et al. 2019), and launches the training using CTDE. Then, when the training stabilizes, recording the sample trajectories in the replay buffer produces the desired dataset, referred to as the expert-level dataset, as the recorded trajectories are generated by the optimal policies with benchmark performance. To diversify the offline data, one can also start recording the sample trajectories midway when the policy displays a medium level of performance. Both expert and medium-level datasets are utilized in our experiments. To facilitate our discussion, we assume that the data collected under CTDE corresponds to the Nash play in the sense that the trajectories follow the equilibrium distribution induced by NE according to the Ionescu-Tulcea extension theorem (Ash and Doléans-Dade 2000, Chapter 2).

**Assumption 1 (CTDE follows NE)** *The sample trajectory in the expert-level dataset  $\tau = \{(s^t, (o_i^t, a_i^t)_{i \in [N]})_{t=1}^T\}$  follows the equilibrium trajectory distribution, denoted by  $q_{NE}$ , comprised of the NE policies  $\pi_i^*$ ,  $i \in [N]$  and the transition kernel  $\mathcal{P}$ .*

We admit that the above is a rather strong assumption. Except for a few value-based algorithms (Hu and Wellman 2003; Greenwald and Hall 2003; Li et al. 2022; Li, Peng, and Zhu 2021) with equilibrium convergence, most policy-based MARL algorithms only prove to be convergent to stationary points (Zhang, Yang, and Başar 2021; Li, Lei, and Zhu 2022). Yet, our key observation is that the resulting benchmark RL policies produced a fixed trajectory distribution corresponding to the stationary point in the offline dataset, which, if imitated, would also suffer the curse of the nonstationary opponent.

### Offline MARL as Sequence Modeling

Inspired by the recent success of Decision Transformer (Chen et al. 2021) and Trajectory Transformer (Janner, Li, and Levine 2022) in dealing with offline (single-agent) RL tasks, there emerges a research thrust trying to extend the transformer to the offline MARL paradigm. At the core of these transformer-based approaches is the treatment of a trajectory as a sequence for modeling by the Transformer architecture (Vaswani et al. 2017). The following takes the multi-agent decision transformer (MADT) in (Meng et al. 2023) as an example to illustrate the connection between offline MARL and sequence modeling.

Consider a trajectory  $\tau$  from the CTDE dataset given by

$$\tau = \{s^1, \mathbf{o}^1, \mathbf{a}^1, s^2, \mathbf{o}^2, \mathbf{a}^2, \dots, s^T, \mathbf{o}^T, \mathbf{a}^T\}. \quad (2)$$

The MADT, parameterized by a decoder network  $q_\phi$ , predicts sequential actions at each time step autoregressively. Let  $\hat{\tau}^t = \{s^1, \mathbf{o}^1, \hat{\mathbf{a}}^1, \dots, s^1, \mathbf{o}^t, \hat{\mathbf{a}}^t\}$  be the truncated trajectory up to time  $t$  with previous action predictions. Then, the MADT’s sequential prediction proceeds as follows.

$$\hat{\mathbf{a}}^t = \arg \max_{\mathbf{a}} q_\theta(\mathbf{a} | \hat{\tau}^{t-1}, s^t, \mathbf{o}^t) \quad (3)$$

The learning objective of the MADT is to minimize the distribution discrepancy between the prediction  $q_\phi$  and the ground truth  $q_{NE}$ . Toward this end, one can consider the cross entropy (CE) loss to train the MADT for discrete cases. Given predictions  $\{\hat{\mathbf{a}}^t\}$ , the CE loss is defined as

$$\mathcal{L}_{CE}(\theta) = 1/T \sum_{t=1}^T q_{NE}(\mathbf{a}^t) \log q_\theta(\hat{\mathbf{a}}^t | \hat{\tau}^{t-1}, s^t, \mathbf{o}^t).$$

For continuous control tasks, the mean-squared error  $\|\hat{\mathbf{a}}^t - \mathbf{a}^t\|^2$  leads to decent transformer policies as observed in (Chen et al. 2021).

## Self-Confirming Transformer

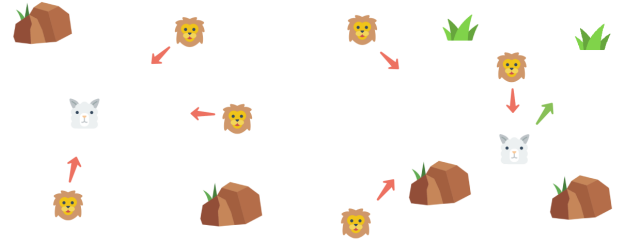
The current explorations of transformer-based offline MARL mainly focus on the cooperative setting, where a central transformer policy, trained using the CTDE dataset, controls every agent in the environment. Alternatively, to achieve decentralized execution, one can first train a teacher transformer using global information and then distill the teacher’s knowledge into a collection of student transformer policies, each of which controls an individual agent (Tseng et al. 2022). Nevertheless, the transformers have full control over agents’ behaviors in a cooperative task.

This work investigates the non-cooperative MARL setting, where some of the agents are beyond the transformer’s control during testing. Such a setting fits human-robot interaction scenarios where the robots act as companions, assistants, or even adversaries (Mutlu, Roy, and Šabanović 2016) of humans who are beyond the robot’s direct control. In such non-cooperative multi-agent environments, chances are that independent agents (opponents) may assume a behavior pattern distinct from what is recorded in the offline dataset. Taking the NE strategy recorded in offline data as the reference point, opponents who employ different strategies during testing are referred to as nonstationary. One naturally wonders whether the transformer policy, controlling a single or a subset of agents, is capable of dealing with such online nonstationarity, as the transformer’s learning objective is only to mimic  $q_{NE}$ . The following numerical example provides a negative answer, demonstrating that the MADT returns a degrading performance when facing a nonstationary opponent.

### The Motivating Example: Nonstationary Opponent

We consider the predator-prey task (a.k.a `simple-tag`) included in the multi-agent particle environment (MPE) (Lowe et al. 2017), one of the benchmark environments in MARL. As shown in Figure 2a, the environment includes a prey who moves faster and aims to evade the three predators. The predators are slower and try to hit the prey, while avoiding obstacles.

The predators observe the relative positions and velocities of the prey, while the prey can only observe the relative positions of the other agents. All agents’ actions are two-dimensional velocity vectors. Each time any one of the three predators collides with the prey, the former gets rewarded while the latter is penalized. The predator-prey is a mixed



(a) `simple-tag`: the three slow-moving predators aim to catch the fast-moving prey while avoiding the obstacles. (b) `simple-world`: a variant of `simple-tag` with two food particles added to the environment. The prey is rewarded when hitting the food.

Figure 2: The predator-prey tasks in multi-agent particle environment.

cooperative-competitive task, where the predators cooperate with each other to encircle the prey so that the rewards get tripled, while the game between the prey and predators is zero-sum like. Another environment we consider is `simple-world` shown in Figure 2b, a more complicated variant of `simple-tag` as it includes 2 food particles that prey is rewarded for being close to. More details on the two environments are included in the appendix.

We here briefly touch upon the training and the testing procedure, while the detailed experiment setup is included in the experiment section and the appendix. We use MATD3 to train the four agents (three predators and one prey) and collect expert-level data, with which the MADT is trained offline. The MADT is trained using offline trajectories of the three predators. The prey employs the following baseline policies during the testing: 1)  $\pi^M$ , the same MATD3 policy used to collect the data; 3)  $\pi^R$ , the random policy; and 4)  $\pi^B$ , a blend of the random and the MATD3 policy. The random policy takes a uniform distribution over the action set regardless of the observation input. The blending policy works like a bang-bang controller: at each time step, the prey flips a coin first; if heads up, then it chooses  $\pi^M$ , otherwise  $\pi^R$ . This blend can be written as  $\pi_B = p \times \pi^M + (1-p) \times \pi^R$ , where the parameter  $p$  is the success probability of the binomial distribution, capturing the opponent’s nonstationarity through the discrepancy between  $\pi^B$  and  $\pi^M$ .

The purpose of this numerical example is to examine the MADT’s online adaptability when facing a nonstationary opponent in testing. Since the nonstationary opponent utilizes a distinct policy, the resulting trajectory deviates from the offline data. This adaptability concerns whether the MADT adjusts its action prediction according to the changing trajectory distribution. The evaluation metric is the normalized score, a customary metric indicating the discounted returns (Fu et al. 2020). The testing results are reported in Figure 3, from which one can see that the MADT’s performance gradually degrades as the opponent deviates from  $\pi^M$ , or equivalently, as the trajectory distribution in testing deviates from  $q_{NE}$ .

Yet, one interesting phenomenon we observe is that the

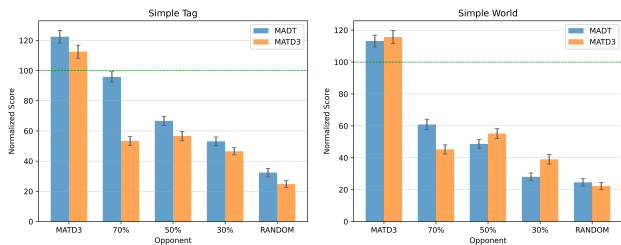


Figure 3: The normalized scores (the higher, the better) of playing the MADT and the MATD3 policy against the nonstationary opponent in simple-tag (left) and simple-world (right). The opponent employs a blend of the benchmark MATD3 and the random policy, with the blending rate  $p$  (shown on the x-axis) chosen from  $\{1, 0.7, 0.5, 0.3, 0\}$ . The smaller  $p$  is, the more discrepant the blending policy is from the offline dataset. The green dashed line indicates the benchmark performance of the testing task.

transformer-based policy does exhibit online adaptability compared with the pre-trained MARL policy, though to a limited extent. We equip the three predators with the MATD3 policies that are used in the data collection and let them play with the three baseline prey policies mentioned above. We denote the predators’ MATD3 policies by  $\pi_{pred}^M$ . Note that  $\pi_{pred}^M$  includes three MATD3 policies and one for each predator. Figure 3 summarizes the testing results, from which one can see that  $\pi_{pred}^M$  gives even lower scores than the MADT does. We believe this adaptability originates from the generalization ability of the transformer architecture, which is also observed in large language models (Radford et al. 2018) and robotic transformers (Reed et al. 2022). This motivating example prompts one to ask: *can transformers learn an adaptable policy from the CTDE dataset that generalizes to non-Nash plays during online testing?* Before answering this question, we first revisit the CTDE practice and the intuition behind NE whose limitation motivates our self-confirming approach.

### Reflection on CTDE and Nash Equilibrium

CTDE, originally designed from online MARL, provides a viable approach to address learning instability in multi-agent environments. With access to global information, each agent can properly evaluate its policy quality conditional on others’ policies based on the centralized critic (a  $Q$ -function of joint actions and observations) (Lowe et al. 2017), leading to an effective policy improvement that finally reaches the equilibrium. When moving to the offline MARL paradigm, without online interactions, the critic receives no updates and is fixed. Consequently, the equilibrium policy  $\pi^*$  associated with this critic can only reproduce the trajectory for the data collection, which follows  $q_{NE}$  as assumed in Assumption 1. The transformer policy trained using this equilibrium data inevitably suffers the distribution shift caused by the nonstationary opponent, as shown in the motivating example. Using game theory language, the transformer agent holds the wrong belief that the opponent is rational and em-

plays an equilibrium policy in testing. This wrong belief is rooted in the centralized critic and, subsequently, the offline data.

From a game-theoretic viewpoint, the curse of nonstationary opponents arises from the *collective rationality* indicated by NE. For any individual agent, employing the equilibrium policy  $\pi_i^*$  is rational, which maximizes the return defined in (1), only if everyone else is rational, i.e., taking the equilibrium policies  $\pi_{-i}^*$ . Had anyone deviated from its equilibrium policy, it would be meaningless for the rest to stick to theirs. Hence, the question to be addressed is how to correct the wrong belief if the opponent violates collective rationality.

### Self-Confirming Equilibrium and Local Consistency

To facilitate the discussion, we introduce the following notations. Given a joint policy  $\pi = (\pi_i, \pi_{-i})$ , the corresponding trajectory distribution is denoted by  $q_\pi$ . An information set  $\mathcal{I}_i^t$  is said to be realizable under  $\pi$  if there exists a trajectory  $\tau$  such that  $\mathcal{I}_i^t \subset \tau$  and  $q_\pi(\tau) > 0$ . In other words,  $\mathcal{I}_i^t$  occurs with strictly positive probability, which is written as  $q_\pi(\mathcal{I}_i^t) > 0$  with a slight abuse of notation. We define  $\mu_i$  as the agent  $i$ ’s conjecture (or belief; the two are used interchangeably) on others’ strategies as a probability measure over  $\Pi_{-i}$ . We denote by  $\hat{\pi}_{-i} = (\hat{\pi}_j)_{j \neq i, j \in [N]}$  to distinguish the subjective conjecture from the true strategies employed by other agents. The following present the self-confirming equilibrium for the POMG adapted from (Fudenberg and Levine 1993, Definition 1).

**Definition 1 (Self-Confirming Equilibrium)** A joint policy  $\pi$  is a self-confirming equilibrium of the POMG if, for each agent  $i$ , there exists a conjecture  $\mu_i$  such that

$$\pi_i \in \arg \max \mathbb{E}_{\hat{\pi}_{-i} \sim \mu_{-i}} \mathbb{E}_{\pi_i, \hat{\pi}_{-i}} \left[ \sum_t \gamma^t r_i^t \right], \quad (4a)$$

$$\mu_i[\{\hat{\pi}_{-i} | \hat{\pi}_j(\mathcal{I}_j^t) = \pi_j(\mathcal{I}_j^t)\}] = 1, \forall j \neq i, q_\pi(\mathcal{I}_j^t) > 0, t \in [T]. \quad (4b)$$

One can see from (4) that SCE embodies subjective rationality, where the agent maximizes its expected utility in (4a) subject to the conjecture of its opponents’ strategies. Such a conjecture is locally consistent in the sense that the probability measure  $\mu_i$  concentrates all probability mass on the joint policy  $\hat{\pi}_{-i}$  that coincides with the true distribution at information sets  $\mathcal{I}_j^t$  that are reached with positive probability. As a comparison, if one drops the positivity condition  $q_\pi(\mathcal{I}_j^t) > 0$ , and the equation in (4b) holds for every possible information set, even those never realize (hence, global), the resulting SCE reduces to NE (Fudenberg and Levine 1993). The key message to be conveyed to the reader through the argument above is that SCE is more flexible than NE: the agent’s decision-making is legitimate as long as there exists a conjecture matching the opponent’s realized actions.

### Self-Confirming Loss

We now articulate how the self-confirming equilibrium helps address the curse of the nonstationary opponent. The following presents the offline training procedure for a self-confirming transformer of an individual agent to ease the

exposition. The proposed method is later extended to controlling multiple agents in the experiment section.

Taking inspiration from SCE, we decompose the agent’s decision-making into belief generation and policy generation. The intuition is that we explicitly equip the agent with a reasoning module that can be trained to conjecture on the opponent’s move online. For belief generation, the agent conjectures the opponent’s future move based on the information set  $\mathcal{I}_i^t$ . Using notations in subsection “Offline MARL as Sequence Modeling,” the conjecture is given by  $\hat{a}_{-i}^t = \mu_i(\mathcal{I}_i^t)$ , which shall match the realized opponent’s action  $a_{-i}^t$ , guaranteeing local consistency. Based on the generated belief, the agent’s policy  $\hat{a}_i^t = \pi_i(\hat{a}_{-i}^t, \mathcal{I}_i^t)$  generates the action  $\hat{a}_i^t$  to be implemented at time  $t$ .

In the offline training phase, we utilize the CTDE data to train the belief and the policy generation model. For simplicity, we consider the continuous-action case and use the mean-squared error. As suggested in (4), the belief generation needs to be locally consistent, and the policy generation is required to be the maximizer. Towards this end, we use the MSE between the opponent’s action in the dataset and the conjecture as the belief loss:  $\|a_{-i}^t - \hat{a}_{-i}^t\|^2$ . As for the policy loss, note that we assume CTDE follows NE plays, and hence, the agent’s optimal actions are exactly those recorded in the dataset. Consequently,  $\|a_i^t - \hat{a}_i^t\|^2$ , the MSE between the agent’s action in the dataset and the generated one gives a substitute to (4a).

Even though SCE introduces this belief generation in addition to the policy generation, one single transformer suffices to represent both, as the two generation processes take a sequential order: the agent first conjecture. Hence, we use a causal transformer (Chen et al. 2021) parameterized by  $\theta_i$  to represent the compound function of the two:  $q_{SC}(\theta_i) = \pi_i \circ \mu_i$ . Consisting of both the belief loss motivated by local consistency (4b) and the policy loss by (4a), the proposed self-confirming loss is as below.

$$\mathcal{L}_{SC}(\theta_i) = \underbrace{\|a_{-i}^t - \hat{a}_{-i}^t\|^2}_{\text{belief loss, (4b)}} + \underbrace{\|a_i^t - \hat{a}_i^t\|^2}_{\text{policy loss, (4a)}}. \quad (5)$$

## Experiments

This section presents a series of experiments to evaluate the online performance of the proposed SCT. Our experiments seek to empirically answer the question we raise at the beginning of this paper: can SCT adapt to nonstationary opponents online? Relatedly, one may wonder whether the offline-trained belief generation produces consistent conjectures online. If so, to what extent, does SCT’s success depend on the conjecture (ablation)?

**Baselines** To address these questions, we conduct a comparative study between SCT and existing approaches based on imitation learning, offline MARL, and sequence modeling. Specifically, we consider the following baselines. The implementation details are in the appendix. **BC**: behavior cloning, an imitation learning algorithm. **MA-BCQ**: multi-agent batch-constrained Q-learning (Fujimoto, Meger, and Precup 2019), which impose constraints on the action space to compel the agent to align more closely with on-policy

behavior regarding a subset of the provided data. **OMAR**: Offline MARL with Actor Rectification (Pan et al. 2022), which uses zeroth-order information to rectify the critic so as to update the actor conservatively. In addition to BCQ and OMAR, there exist many other competitive baselines, such as CQL (Kumar et al. 2020) and ICQ (Yang et al. 2021). However, it is reported in (Pan et al. 2022) that OMAR outperforms CQL and ICQ in the MPE environments considered in this paper, i.e., the simple-tag and simple-world environments to be introduced later. Hence, we pick MA-BCQ, which is not included in (Pan et al. 2022), as the representative offline MARL algorithm to be evaluated, in addition to OMAR. Finally, we consider transformer-based models for the ablation studies, which include the **MADT** discussed in the motivating example and **Conjectural-MADT (CMADT)**, a variant of MADT we construct with the training loss augmented by the belief loss. The connections among the three transformer models (including SCT) are highlight in the ablation part.

**Environments and Offline Dataset** In accordance with the benchmarking testbed in the literature, e.g., (Pan et al. 2022; Tseng et al. 2022), we consider `simple-tag` and `simple-world` discussed in the motivating example. The detailed environment setup is in the appendix. Our SCT and the baseline algorithms are trained using the offline dataset offered by (Pan et al. 2022). Slightly different from the representation in (2), the trajectory in the dataset takes the following form:  $\tau = \{\hat{R}_i^t, (o_i^t)_{i \in [N]}, (a_i^t)_{i \in [N]}\}$ , where the reward  $r_i^t$  is replaced by the reward-to-go  $\hat{R}_i^t := \sum_{k=t}^T r_i^k$ . Such a rearrangement follows the practice in (Chen et al. 2021), equipping the agent with forward-looking. The offline trajectories representing random, medium, and expert levels of play are divided into three datasets, where each dataset consists of 1 million transitions. The random dataset is obtained from unrolling episodes of a randomly initialized policy. The medium dataset is obtained from early stopping the training phase of a MATD3 algorithm once it reaches a medium level of play, and then unrolling the episodes. The final dataset is given by collecting transitions from the MATD3 algorithm once it is fully trained.

**Nonstationary Opponent** To evaluate the adaptability of the predators, the prey is controlled by five distinct policies for each task. These opponent policies include 1) the **MATD3** policy, the one used to collect the training data, 2) **MADDPG** policy, an actor-critic policy trained for each environment, 3) **Random** policy: a heuristic-based policy designed to randomly sample feasible actions, 4) **Still** policy: a simple policy that freezes the prey at the initialized location, 5) **Blend** policy, the blending policy introduced in the motivating example with 50% blending rate.

**Quantitive Results** First, to complete the story in the motivating example, we add SCT’s normalized scores to the bar plots in Figure 3, leading to Figure 4. The figure suggests that SCT adapts better to nonstationary opponents in testing than MADT. Due to the page limit, we mainly report the experimental results of `simple-tag`, and those of `simple-world` are deferred to the appendix, as they display similar patterns. For all the experiments,

Table 1: The normalized scores of SCT and baseline algorithms trained under the expert, medium, and random datasets. SCT exhibits greater online adaptability than those baselines.

	Simple-Tag	MATD3 prey	MADDPG prey	Still prey	Random prey	Blend prey
Expert	OMAR	103.19 ± 8.29	9.05 ± 1.62	38.80 ± 7.54	24.13 ± 4.08	58.02 ± 4.95
	BC	121.11 ± 7.81	11.22 ± 3.24	44.57 ± 6.8	35.7 ± 4.95	73.65 ± 5.04
	MA-BCQ	113.92 ± 8.16	10.52 ± 1.52	31.67 ± 6.83	31.26 ± 5.25	67.39 ± 5.97
	MADT	123.32 ± 8.04	8.16 ± 1.57	44.10 ± 7.9	32.83 ± 5.48	76.90 ± 5.23
	CMADT	122.94 ± 4.50	7.53 ± 1.80	32.52 ± 2.74	38.28 ± 4.29	70.04 ± 20.87
	SCT	<b>126.20 ± 7.48</b>	<b>11.94 ± 1.79</b>	<b>54.87 ± 7.54</b>	<b>38.98 ± 4.97</b>	<b>92.87 ± 5.92</b>
Medium	OMAR	72.61 ± 6.69	10.78 ± 1.21	42.49 ± 6.67	24.68 ± 3.73	44.14 ± 4.78
	BC	77.49 ± 6.93	11.60 ± 2.72	43.20 ± 6.39	31.41 ± 4.11	54.05 ± 4.35
	MA-BCQ	56.08 ± 6.05	10.36 ± 1.39	33.75 ± 6.27	25.65 ± 3.98	49.51 ± 4.6
	MADT	73.96 ± 5.76	11.98 ± 1.60	37.81 ± 5.96	27.58 ± 4.05	50.47 ± 4.42
	CMADT	74.67 ± 3.5	8.90 ± 1.31	29.21 ± 1.93	<b>50.77 ± 3.46</b>	44.15 ± 2.10
	SCT	<b>79.33 ± 5.80</b>	<b>12.22 ± 1.55</b>	<b>52.87 ± 6.02</b>	34.78 ± 3.52	<b>61.54 ± 5.05</b>
Random	OMAR	6.71 ± 3.03	-1.48 ± 0.43	1.53 ± 2.06	1.50 ± 1.11	3.53 ± 1.51
	BC	-0.31 ± 1.13	-3.27 ± 0.94	-1.48 ± 0.86	-1.48 ± 1.09	0.03 ± 1.08
	MA-BCQ	<b>32.86 ± 5.73</b>	<b>3.79 ± 1.16</b>	<b>28.1 ± 6.94</b>	<b>6.18 ± 2.94</b>	<b>12.9 ± 3.16</b>
	MADT	9.94 ± 2.56	-0.23 ± 0.63	4.31 ± 2.01	3.07 ± 1.49	4.97 ± 1.65
	CMADT	8.76 ± 1.36	-2.43 ± 0.20	3.44 ± 1.23	0.71 ± 4.25	4.93 ± 0.88
	SCT	24.75 ± 2.73	-0.03 ± 0.78	6.36 ± 1.73	5.03 ± 1.51	6.37 ± 1.57

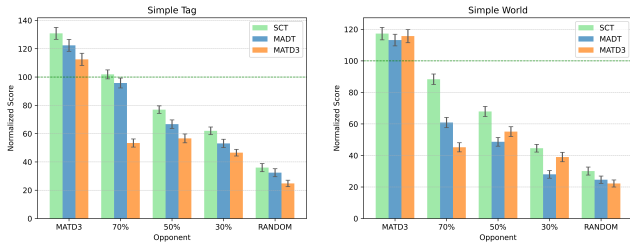


Figure 4: The normalized scores of SCT in simple-tag and simple-world environments. SCT outperforms MADT when facing nonstationary opponents.

we report in Table 1 the mean and standard deviation of normalized scores based on 100 runs using different random seeds. We observe that SCT consistently outperforms both MA-BCQ and OMAR across all experiments, except for the random dataset case where MA-BCQ leads extensively. Furthermore, SCT’s performance is on par with or superior to the BC approach. Notably, SCT exhibits greater adaptability compared to its basic counterpart, as indicated by higher mean rewards in most experiments.

**Ablation** We compare SCT with MADT and CMADT to see to what extent the belief generation contributes to the SCT’s success. MADT is trained to generate predators’ action using the predators’ offline trajectories without any conjecture on the prey. In contrast, CMADT also learns to reason the opponent’s move. Similar to (3), its sequential generation is  $\hat{a}_{prey}^t, \hat{a}_{pred}^t = \arg \max_{\mathbf{a}} q_{\theta}(\mathbf{a} | \hat{\tau}^{t-1}, o_{pred}^t)$  and the associated loss follows  $\mathcal{L}(\theta) = \|\hat{a}_{prey}^t - a_{prey}^t\|^2 + \|\hat{a}_{pred}^t - a_{pred}^t\|^2$ . What distinguishes SCT from CMADT is that CMADT outputs the con-

Table 2: The prediction accuracy of SCT and CMADT in simple-tag.

		Accuracy	MATD3	MADDPG	Still	Random	Blend
Exp	SCT	1.000	0.086	0.978	0.310	0.803	
	CMADT	1.000	0.092	0.980	0.292	0.780	
Med	SCT	1.000	0.095	0.996	0.300	0.888	
	CMADT	1.000	0.116	0.988	0.324	0.872	
Rand	SCT	1.000	0.217	1.000	0.301	0.865	
	CMADT	1.000	0.204	1.000	0.308	0.792	

jecture  $\hat{a}_{prey}^t$  and the action  $\hat{a}_{pred}^t$  simultaneously based on past observations, whereas SCT first generates the conjecture that later serves as the input to the action generation, see Figure 1 for visualization of SCT (CMADT is visualized in the appendix). Intuitively, the belief generation is equally important as the policy generation in SCT, considering the transformer’s sequence-modeling nature. While in CMADT, the belief generation barely regularizes the policy generation, which is referred to as belief regularization. We record the opponent’s action prediction accuracy of SCT and CMADT in simple-tag testing, which indicates the number of steps over an episode at which is prediction is close to the truth (the exact definition is in the appendix). As shown in Table 2, SCT and CMADT return comparable results, suggesting that the two acquire similar forecasting abilities. Hence, the superiority of SCT, as indicated in Table 1, shows that belief generation plays a bigger part than regularization, validating the self-confirming intuition.

## References

- Ackermann, J.; Gabler, V.; Osa, T.; and Sugiyama, M. 2019. Reducing overestimation bias in multi-agent domains using double centralized critics. *arXiv preprint arXiv:1910.01465*.
- Ash, R. B.; and Doléans-Dade, C. 2000. *Probability and Measure Theory*. Academic Press. Academic Press. ISBN 9780120652020.
- Bannon, J.; Windsor, B.; Song, W.; and Li, T. 2020. Causality and Batch Reinforcement Learning: Complementary Approaches To Planning In Unknown Domains. *arXiv preprint arXiv:2006.02579*.
- Chen, L.; Lu, K.; Rajeswaran, A.; Lee, K.; Grover, A.; Laskin, M.; Abbeel, P.; Srinivas, A.; and Mordatch, I. 2021. Decision transformer: Reinforcement learning via sequence modeling. *Advances in neural information processing systems*, 34: 15084–15097.
- Foerster, J.; Farquhar, G.; Afouras, T.; Nardelli, N.; and Whiteson, S. 2018. Counterfactual multi-agent policy gradients. In *Proceedings of the AAAI conference on artificial intelligence*, volume 32.
- Fu, J.; Kumar, A.; Nachum, O.; Tucker, G.; and Levine, S. 2020. D4rl: Datasets for deep data-driven reinforcement learning. *arXiv preprint arXiv:2004.07219*.
- Fudenberg, D.; and Levine, D. K. 1993. Self-Confirming Equilibrium. *Econometrica*, 61(3): 523.
- Fujimoto, S.; and Gu, S. S. 2021. A minimalist approach to offline reinforcement learning. *Advances in neural information processing systems*, 34: 20132–20145.
- Fujimoto, S.; Meger, D.; and Precup, D. 2019. Off-policy deep reinforcement learning without exploration. In *International conference on machine learning*, 2052–2062. PMLR.
- Greenwald, A.; and Hall, K. 2003. Correlated-Q Learning. In *Proceedings of the Twentieth International Conference on Machine Learning*, volume 20 of *ICML'03*, 242.
- Hu, J.; and Wellman, M. P. 2003. Nash Q-learning for general-sum stochastic games. *Journal of machine learning research*, 4(Nov): 1039–1069.
- Janner, M.; Li, Q.; and Levine, S. 2022. Offline Reinforcement Learning as One Big Sequence Modeling Problem. In *Advances in Neural Information Processing Systems*, volume 34, 1273–1286. Curran Associates, Inc.
- Kumar, A.; Zhou, A.; Tucker, G.; and Levine, S. 2020. Conservative q-learning for offline reinforcement learning. *Advances in Neural Information Processing Systems*, 33: 1179–1191.
- Károly, A. I.; Galambos, P.; Kuti, J.; and Rudas, I. J. 2021. Deep Learning in Robotics: Survey on Model Structures and Training Strategies. *IEEE Transactions on Systems, Man, and Cybernetics: Systems*, 51(1): 266–279.
- Levine, S.; Kumar, A.; Tucker, G.; and Fu, J. 2020. Offline Reinforcement Learning: Tutorial, Review, and Perspectives on Open Problems. *arXiv*.
- Li, T.; Lei, H.; and Zhu, Q. 2022. Sampling Attacks on Meta Reinforcement Learning: A Minimax Formulation and Complexity Analysis. *arXiv preprint arXiv:2208.00081*.
- Li, T.; Lei, H.; and Zhu, Q. 2023. Self-Adaptive Driving in Non-stationary Environments through Conjectural Online Lookahead Adaptation. *2023 IEEE International Conference on Robotics and Automation (ICRA)*, 00: 7205–7211.
- Li, T.; Peng, G.; and Zhu, Q. 2021. Blackwell Online Learning for Markov Decision Processes. *2021 55th Annual Conference on Information Sciences and Systems (CISS)*, 00: 1–6.
- Li, T.; Peng, G.; Zhu, Q.; and Baar, T. 2022. The Confluence of Networks, Games, and Learning a Game-Theoretic Framework for Multiagent Decision Making Over Networks. *IEEE Control Systems*, 42(4): 35–67.
- Li, T.; Zhao, Y.; and Zhu, Q. 2022. The role of information structures in game-theoretic multi-agent learning. *Annual Reviews in Control*, 53: 296–314.
- Li, T.; and Zhu, Q. 2019. On Convergence Rate of Adaptive Multi-scale Value Function Approximation for Reinforcement Learning. *2019 IEEE 29th International Workshop on Machine Learning for Signal Processing (MLSP)*, 1–6.
- Lowe, R.; WU, Y.; Tamar, A.; Harb, J.; Abbeel, O. P.; and Mordatch, I. 2017. Multi-Agent Actor-Critic for Mixed Cooperative-Competitive Environments. In *Advances in Neural Information Processing Systems 30*, Advances in Neural Information Processing Systems, 6379–6390. Curran Associates, Inc.
- Meng, L.; Wen, M.; Le, C.; Li, X.; Xing, D.; Zhang, W.; Wen, Y.; Zhang, H.; Wang, J.; Yang, Y.; and Xu, B. 2023. Offline Pre-trained Multi-agent Decision Transformer. *Machine Intelligence Research*, 20(2): 233–248.
- Mutlu, B.; Roy, N.; and Šabanović, S. 2016. Springer Handbook of Robotics. *Springer Handbooks*, 1907–1934.
- Nash, J. 1951. Non-Cooperative Games. *The Annals of Mathematics*, 54(2): 286–295.
- Pan, L.; Huang, L.; Ma, T.; and Xu, H. 2022. Plan better amid conservatism: Offline multi-agent reinforcement learning with actor rectification. In *International Conference on Machine Learning*, 17221–17237. PMLR.
- Radford, A.; Narasimhan, K.; Salimans, T.; Sutskever, I.; et al. 2018. Improving language understanding by generative pre-training.
- Rashid, T.; Samvelyan, M.; De Witt, C. S.; Farquhar, G.; Foerster, J.; and Whiteson, S. 2020. Monotonic value function factorisation for deep multi-agent reinforcement learning. *The Journal of Machine Learning Research*, 21(1): 7234–7284.
- Reed, S.; Zolna, K.; Parisotto, E.; Colmenarejo, S. G.; Novikov, A.; Barth-maroon, G.; Giménez, M.; Sulsky, Y.; Kay, J.; Springenberg, J. T.; et al. 2022. A Generalist Agent. *Transactions on Machine Learning Research*.
- Sunehag, P.; Lever, G.; Grusl, A.; Czarnecki, W. M.; Zambaldi, V.; Jaderberg, M.; Lanctot, M.; Sonnerat, N.; Leibo, J. Z.; Tuyls, K.; and Graepel, T. 2018. Value-Decomposition Networks For Cooperative Multi-Agent Learning Based On Team Reward. In *Proceedings of the 17th International Conference on Autonomous Agents and MultiAgent Systems*, AAMAS '18, 2085–2087. Richland, SC: International Foundation for Autonomous Agents and Multiagent Systems.
- Sutton, R. S.; Maei, H. R.; and Szepesvári, C. 2009. A Convergent  $O(n)$  Temporal-difference Algorithm for Off-policy Learning with Linear Function Approximation. *Advances in Neural Information Processing Systems*, 1609–1616.
- Tseng, W.-C.; Wang, T.-H. J.; Lin, Y.-C.; and Isola, P. 2022. Offline Multi-Agent Reinforcement Learning with Knowledge Distillation. In *Advances in Neural Information Processing Systems*, volume 35, 226–237. Curran Associates, Inc.
- Vaswani, A.; Shazeer, N.; Parmar, N.; Uszkoreit, J.; Jones, L.; Gomez, A. N.; Kaiser, L.; and Polosukhin, I. 2017. Attention is All you Need. In *Advances in Neural Information Processing Systems*, volume 30 of *NeurIPS*. Curran Associates, Inc.
- Wen, M.; Kuba, J.; Lin, R.; Zhang, W.; Wen, Y.; Wang, J.; and Yang, Y. 2022. Multi-Agent Reinforcement Learning is a Sequence Modeling Problem. In *Advances in Neural Information Processing Systems*, volume 35, 16509–16521. Curran Associates, Inc.



Yang, Y.; Ma, X.; Li, C.; Zheng, Z.; Zhang, Q.; Huang, G.; Yang, J.; and Zhao, Q. 2021. Believe What You See: Implicit Constraint Approach for Offline Multi-Agent Reinforcement Learning. In *Neural Information Processing Systems*.

Yu, C.; Liu, J.; Nemati, S.; and Yin, G. 2021. Reinforcement Learning in Healthcare: A Survey. *ACM Comput. Surv.*, 55(1).

Zhang, K.; Yang, Z.; and Başar, T. 2021. Multi-agent reinforcement learning: A selective overview of theories and algorithms. *Handbook of reinforcement learning and control*, 321–384.

## Transformer Architecture

The transformer architecture (Vaswani et al. 2017) has shown outstanding generalization capabilities in natural language processing (Radford et al. 2018). Its success is mainly due to the model’s attention block, which effectively captures long-range temporal dependencies.

The raw inputs of the transformer (which we will call tokens) are initially embedded to vectors of dimension  $d_{model}$ . Each input embedding generates a query, key, and value vector of dimensions  $d_q$ ,  $d_k$ , and  $d_v$ . Vectors of the same type are stacked column-wise to produce three matrices  $Q \in \mathbb{R}^{l \times d_q}$ ,  $K \in \mathbb{R}^{l \times d_k}$ , and  $V \in \mathbb{R}^{l \times d_v}$ , with  $l$  the maximum context length (i.e., the length of the input sequence, defined as a hyperparameter). The attention score is then calculated with the formula

$$\text{Attention}(Q, K, V) = \text{softmax} \left( \frac{QK^T}{\sqrt{d_k}} \right) V.$$

The matrix  $QK^T$  is divided by  $\sqrt{d_k}$  to prevent the vanishing gradient problem when applying the soft-max row-wise (Vaswani et al. 2017). After the soft-max computation, the upper off-diagonal triangle part of the resulting matrix  $\text{softmax}(QK^T/\sqrt{d_k}) \in \mathbb{R}^{l \times l}$  is masked with 0s. This causal mask prevents future tokens from influencing the prediction of the current target, and is the defining feature of a **causal transformer**, distinctive from other variations.

It is common practice in transformer research to divide the attention into several, smaller heads, to later concatenate them in the final attention score. This strategy, called "multi-head attention," (Vaswani et al. 2017) however, is not incorporated in our self-confirming transformer model, as we didn’t observe any performance enhancement through its implementation.

Another essential component of the transformer architecture is the feed-forward neural network preceding the attention mechanism. The computation is as follows.

$$\text{FFN}(\mathbf{x}) = (\max(0, \mathbf{x} \cdot \mathbf{W}_1 + \mathbf{b}_1)) \cdot \mathbf{W}_2 + \mathbf{b}_2,$$

where  $W_1 \in \mathbb{R}^{d_v \times d_f}$  and  $W_2 \in \mathbb{R}^{d_f \times d_{model}}$  are the weights, and  $b_1 \in \mathbb{R}^{d_f}$  and  $b_2 \in \mathbb{R}^{d_{model}}$  are the biases, with  $d_f = 4d_k$ . The input of this network is the computed attention score.

Note that all of the operations above are permutation invariant, so to consider the sequential and time-dependent nature of the data, we inject positional encoding learned as an embedding table to the input embeddings.

A causal transformer block comprises layer normalization, an attention module featuring causal masking, and a feed forward neural network, applied in sequence. A causal transformer typically incorporates more than one of these blocks, where the output of one block serves as the input for the subsequent block. We refer to each column of the matrix returned by the final transformer block as a **hidden state**, denoted by the pre-subscript  $h$ . This matrix is of size  $d_v \times l$ . Each transformer hidden state can be one-to-one mapped to an input token, following the order of the original sequence. Hence, we write  $h a_t^i$  to denote the hidden state that is in the same position

as  $a_t^i$  in the original input sequence. Thanks to the causal masking, each hidden state only contains information preceding that token.

## Environments

Our experiments adopt the Multi-Agent Particle Environment (MPE) (Lowe et al. 2017) to evaluate the proposed SCT. We import two tasks from MPE, which are simple-tag and simple-world. These two environments are very interesting because they capture elements of both competition (between good agents and adversaries) and collaboration (among the good agents themselves to avoid being tagged). The following gives more details about these two environments.

### Simple-Tag

Simple-tag includes three entities: the prey, the predator, and the obstacle. The ensuing discussion presents the environment setup, including the observation, action, and reward of each entity.

The partial observation of the prey contains its own velocity and position, and its relative positions to obstacles and other agents. The action variable of the prey is a two-dimensional vector, each entry of which ranges from -1 to 1. As the prey aims to escape from predators, it gets a positive reward proportional (the factor is 0.1) to the sum of its distance from each predator, while it is penalized for being caught by any of the predators (-10 reward). Since the prey moves faster than predators, to keep the game balanced, it is penalized for being out of the map. The purpose of introducing such a penalty is to prevent the prey from moving in one direction without any restriction.

The partial observation of one predator consists of its own velocity and position, its relative positions to the obstacles and other agents, and the prey’s velocity. The predator’s action space is the same as the prey’s. The predator is rewarded +10 after hitting the prey, otherwise penalized by the relative distance to the prey.

The obstacles are introduced to complicate the environment. Observable to all agents, obstacles are stationary once initialized within an episode. As its name suggests, agents cannot move through the obstacle, which requires them to maneuver strategically around these obstacles to evade (the prey) or ambush (the predator).

We set one prey, three predators, and two obstacles in this environment. Consequently, the observation space of prey is 14-dimensional: 2 for its velocity, 2 for its position, 4 for the relative position to obstacles, and 6 for other relative positions to agents. Similarly, the observation space of predators is 16-dimensional, and the additional 2 entries correspond to the prey’s velocity.

### Simple-World

Simple-world is a more challenging variation of the previous environment. In this scenario, there are additional food particles that the prey is rewarded for being close to. Each predator receives a reward of +5 if one of them hits the prey. On the contrary, the prey is penalized by -5 for each collision. Simple-world relies on the same reward setup as simple-tag. Additionally, the prey is rewarded +2 points for every time it hits a food particle. The environment includes only one obstacle. For the two environments, the episode length is  $T = 25$ . Yet, when training the transformer models, the context length is 20, i.e., the past 20 steps are used to calculate the loss.

## Implementations Details: Training and Testing

This section presents the detailed experiment setup, and the associated source code are included in the supplementary material.

Table 3: Self-confirming transformer hyperparameters

Hyperparameter	Value
Maximum context Length	20
Batch Size	64
Hidden Dimensions	128
# of Layers	3
# of Attention Heads	1
Activation function	ReLU
Dropout	0.1
# Steps per epoch	10000
# Warmup Steps	10000
Epochs	1 for Medium and Expert 10 for Random
Learning Rate	1e-4
Weight Decay	1e-4

### Self-Confirming Transformer

As shown in Figure 5, SCT receives the predators’ observations ( $o_{1:3}^t$ ) and actions ( $a_{1:3}^t$ ) and the rewards-to-go signal ( $\hat{R}^t$ ) as input at each time step. To account for the different dimensions of the input, actions, states, and rewards-to-go are embedded by different linear layers. Then, we introduce positional encoding using a learned embedding table to encode the time-step, so that transformer knows the order of the input. These tokens are then fed into a causal transformer, generating hidden states for each input token.

The hidden states corresponding to the observations are concatenated and sent through a linear layer that predicts the opponent’s actions. During training, this actions is trained via MSE loss with the dataset as ground truth. During testing time, we are not going to use ground truth (the opponent’s action) as input, instead, we just trust the predicted action, and take it as a new component of our input stream.

This process of embedding, encoding, and hidden state generation is repeated, in auto-regressive fashion. For each agent, we concatenate the hidden state related to its observation with the hidden state of the opponent’s predicted action. This concatenated input is then passed through a linear layer, converting it into the agent’s own action. This is carried out for each predator. We note that the concatenation step makes explicit the self-confirming nature of the model. The hyperparameters are summarized in Table 3.

### BC

We implement the Behavior Cloning to imitate the three predators behavior recorded in the dataset. It consists of a Multilayer Perceptron with ReLU activation and dropout. The input consists of the 3 predator’s observation history concatenated and flattened. Since our context-length is 20, the network’s inputs are  $20 \times 16 \times 3 = 960$ -dimensional for simple tag and  $20 \times 24 \times 3 = 1440$ -dimensional for simple-world. The output are 6 dimensional (three 2-dimensional actions). We utilize Mean Squared Error (MSE) loss during training, with dataset’s actions as ground truth. The hyperparameters are summarized in Table 4.

### MA-BCQ

We implement MA-BCQ based on the BCQ implementation provided by (Yang et al. 2021). Considering the fact that BCE employs two Q networks for a single-agent, MA-BCQ includes six Q networks as each predator needs two critics. The QMixer network in

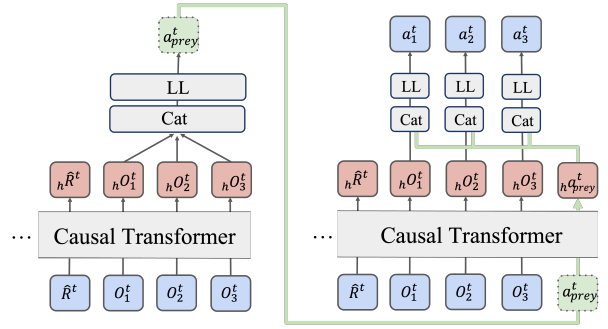


Figure 5: In SCT’s multi-agent implementation, the three predators’ observation hidden states  $h_o_{1,h}^t, h_o_{2,h}^t, h_o_{3,h}^t$  are concatenated (Cat) and passed through a linear layer (LL) to predict the opponent’s action (the green block), which becomes part of the input stream. Then, the prey’s action hidden state  $h_a_{prey}^t$  is concatenated with the corresponding  $h_o_i^t$  and passed through a linear layer for each predator’s action generation.

Table 4: Behavior Cloning hyperparameters

Hyperparameter	Value
Maximum Context Length	20
Batch Size	64
Hidden Dimensions	128
# of Layers	3
Activation Function	ReLU
Dropout	0.1
# Steps per Epoch	10000
# Linear Warm-up Steps	10000
Epochs	15
Learning Rate	1e-4
Weight Decay	1e-4

MA-BCQ takes in six Q values and outputs one Q value to evaluate the joint actions of predators.

In the training, we calculate the Q-target value with Q values given by critic-target and calculate Q-current with Q values given by the critic-current, and then, we obtain the following loss:

$$\mathcal{L}_Q^{BCQ}(\phi, \psi) = \mathbb{E}_{\tau \sim B, \mathbf{a} \sim \mu} [(\tau(\tau, \mathbf{a}) + \gamma \max_{\tilde{\mathbf{a}}^{[j]}} Q^\pi(\tau', \tilde{\mathbf{a}}^{[j]}; \phi', \psi') - Q^\pi(\tau, \mathbf{a}; \phi, \psi))^2],$$

$$\tilde{\mathbf{a}}^{[j]} = \mathbf{a}^{[j]} + \xi(\tau, \mathbf{a}^{[j]}),$$

where  $\phi$  means the parameter of Q network, and  $\psi$  represents the parameters of Mixer network, the  $\xi(\tau, \mathbf{a}^{[j]})$  represents the perturbation model. We follow the hyperparameter setup in (Fujimoto, Meger, and Precup 2019).

### OMAR

We follow the official implementation of OMAR offered by the authors (Pan et al. 2022).

### Ablation Baselines Explained

In order to validate the self-confirming equilibrium intuition behind our proposed model, we compare the performance of SCT

with two transformer-based models, namely (offline) Multiagent Decision Transformer (MADT) and Conjectural Multiagent Decision Transformer (CMADT). Their details are presented below. To better illustrate their differences from and connection to the SCT structure, we provide visualizations of MADT and CMADT in Figure 6 and Figure 7, respectively.

### MADT

The MADT (Meng et al. 2023) is akin to the original Decision Transformer (Chen et al. 2021), in that it takes agent’s observations and rewards-to-go signals as inputs, generating actions in autoregressive fashion. Particularly, in this architecture the opponents actions are not considered neither during training nor testing, so it is not equipped with tools for self-confirming play. Its hyperparameters are the same as those of SCT, summarized in Table 3.

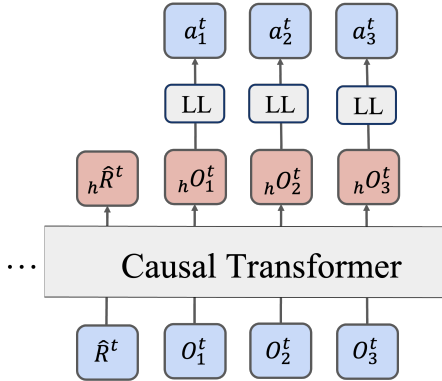


Figure 6: In MADT, the opponent’s actions are not considered neither in training nor inference. Instead, we directly generate the actions from the predators’ observation hidden states  $hO_{1:3}^t$ .

### CMADT

We propose the Conjectural Multiagent Decision Transformer (CMADT). This architecture takes as inputs predators’ observation and action history and the rewards-to-go signal. In a forward pass of this architecture, the opponent’s and the agents actions are predicted in parallel, contrary to our SCT, where the opponent’s conjectured action and agents’ actions decision happen in sequence. The opponent’s conjectured action becomes part of the context for future actions, but is not considered for the current decision process; hence, the self-confirming nature of this model is limited.

### Additional Results

This section reports experiments conducted on simple-world, and the results are summarized in Table 6. We observe that SCT displays higher adaptability than it does in simple-tag. SCT still outperforms all baselines when trained on the expert and medium data, as it does in simple-tag environment. Figure 8 presents the associated bar plots. Furthermore, the SCT trained with random data adapts more effectively to the MATD3, MADDPG, and the random prey than its counterpart in simple-tag (see Table 1). Only under the still and blend prey cases do MA-BCQ and CMADT claim an upper-hand, respectively.

Similar to the ablation study presented in Table 1, we compare SCT and CMADT regarding the opponent’s action prediction. Before presenting the result, we first give an exact definition on the prediction accuracy. We regard an opponent’s action prediction  $\hat{a}_{-i}^t$

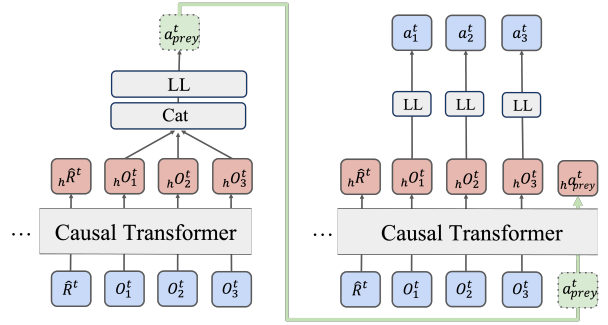


Figure 7: In CMADT, the opponent’s actions are inferred similarly to our SCT, but  $h a_{prey}^t$  is not considered for action generation at timestep  $t$ . It becomes part of the context for future actions.

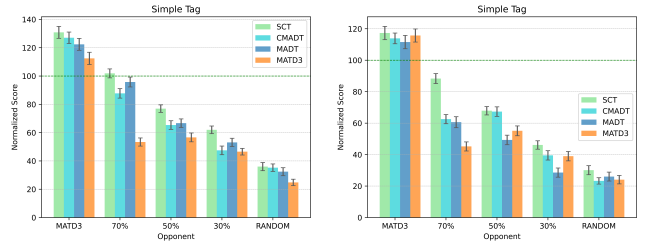


Figure 8: The normalized scores of SCT in simple-tag and simple-world environments. SCT outperforms MADT and CMADT when facing nonstationary opponents.

accurate if it falls within an  $\epsilon$ -neighborhood of the ground truth:  $\hat{a}_{-i}^t \in \{a : \|a - a_{-i}^t\| < \epsilon\}$ . The prediction accuracy of an episode indicates the number of steps at which the prediction is accurate.

$$\text{Accuracy} = \frac{\# \text{steps with accurate predictions}}{\# \text{total steps}}$$

Table 5 summarizes prediction accuracy in the simple-world. We observe patterns similar to Table 1. SCT produces decent predictions for the MATD3 and Still preys, and its prediction accuracy generally matches the blending rate when playing against the Blend prey. Nevertheless, CMADT and SCT acquires indistinguishable prediction abilities, and hence, the success of SCT is rooted in the self-confirming intuition.

Table 5: The prediction accuracy in simple-world experiments.

		Accuracy	MATD3	MADDPG	Still	Random	Blend
Exp	SCT	1.000	0.082	1.000	0.285	0.713	
	CMADT	1.000	0.088	1.000	0.282	0.661	
Med	SCT	1.000	0.102	1.000	0.293	0.650	
	CMADT	1.000	0.088	1.000	0.229	0.577	
Ran	SCT	1.000	0.092	1.000	0.285	0.707	
	CMADT	0.998	0.082	1.000	0.294	0.657	

Table 6: The normalized scores of SCT and baseline algorithms trained under the expert, medium, and random datasets. SCT exhibits greater online adaptability than those baselines in most simple-world experiments.

	Simple World	MATD3 prey	MADDPG prey	Still prey	Random prey	Blend prey
Expert	OMAR	$114.26 \pm 3.52$	$-4.29 \pm 8.33$	$34.52 \pm 3.76$	$23.58 \pm 2.21$	$48.33 \pm 2.82$
	BC	$111.08 \pm 3.12$	$-9.05 \pm 6.10$	$37.73 \pm 3.68$	$25.31 \pm 2.16$	$53.14 \pm 2.52$
	MA-BCQ	$106.59 \pm 3.38$	$-2.75 \pm 6.79$	$45.33 \pm 2.96$	$21.62 \pm 1.63$	$51.07 \pm 2.81$
	MADT	$105.83 \pm 3.18$	$-2.85 \pm 6.76$	$31.69 \pm 3.33$	$23.34 \pm 21.3$	$48.61 \pm 2.66$
	CMADT	$110.44 \pm 3.42$	$-1.54 \pm 7.70$	$41.76 \pm 3.98$	$23.69 \pm 2.13$	$75.90 \pm 3.58$
	SCT	<b><math>115.20 \pm 3.38</math></b>	<b><math>-1.32 \pm 7.15</math></b>	<b><math>53.31 \pm 3.39</math></b>	<b><math>28.28 \pm 2.29</math></b>	<b><math>92.87 \pm 5.92</math></b>
Medium	OMAR	$73.81 \pm 4.46$	$-0.84 \pm 7.23$	<b><math>58.67 \pm 3.73</math></b>	$31.37 \pm 1.73$	$42.23 \pm 2.55$
	BC	$86.23 \pm 2.39$	$-5.48 \pm 10.47$	$41.11 \pm 3.38$	$29.84 \pm 2.06$	$43.45 \pm 2.32$
	MA-BCQ	$76.99 \pm 3.31$	$-3.00 \pm 9.88$	$36.02 \pm 3.71$	$30.12 \pm 1.99$	$40.92 \pm 2.38$
	MADT	$81.70 \pm 2.84$	$0.54 \pm 6.51$	$28.92 \pm 2.82$	$26.07 \pm 1.95$	$43.32 \pm 2.22$
	CMADT	$86.87 \pm 2.93$	$0.96 \pm 8.11$	$30.25 \pm 3.79$	$28.52 \pm 2.13$	$55.78 \pm 2.92$
	SCT	<b><math>87.13 \pm 2.97</math></b>	<b><math>1.30 \pm 5.51</math></b>	$33.41 \pm 3.02$	<b><math>31.87 \pm 1.96</math></b>	<b><math>57.87 \pm 2.66</math></b>
Random	OMAR	$8.37 \pm 1.16$	$-5.51 \pm 0.87$	$4.54 \pm 1.01$	$5.41 \pm 0.77$	$6.39 \pm 0.85$
	BC	$-0.62 \pm 0.62$	$-13.41 \pm 5.28$	$-0.75 \pm 0.58$	$0.06 \pm 0.69$	$0.15 \pm 0.68$
	MA-BCQ	$6.52 \pm 1.42$	<b><math>-3.11 \pm 7.98</math></b>	<b><math>6.59 \pm 1.38</math></b>	$3.40 \pm 0.81$	$4.01 \pm 0.85$
	MADT	$5.28 \pm 1.10$	$-7.21 \pm 5.87$	$1.27 \pm 0.96$	$4.85 \pm 0.89$	$4.28 \pm 0.80$
	CMADT	$8.36 \pm 1.27$	$-7.54 \pm 5.96$	$2.93 \pm 1.01$	$4.61 \pm 0.82$	<b><math>8.12 \pm 0.93</math></b>
	SCT	<b><math>8.95 \pm 1.42</math></b>	$-4.47 \pm 5.80$	$4.93 \pm 0.81$	<b><math>6.09 \pm 0.91</math></b>	$6.37 \pm 1.57$